AD-A131 301 PHOTOLUMINESCENT PROPERTIES OF N-GAAS ELECTRODES: APPLICATIONS OF THE DEA..(U) WISCONSIN UNIV-MADISON DEPT OF CHEMISTRY W S HOBSON ET AL. 26 JUL 83 1/1

UNCLASSIFIED UWIS/DC/TR-83-2 N00014-78-C-0633 F/G 20/12 NL

END
DATE
FILMED
8 83
DTIC

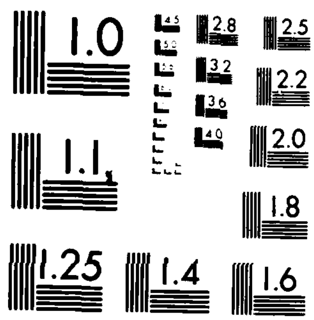

MICROCOPY RESOLUTION TEST CHART
NATIONAL BUREAU OF STANDARDS-1963-A

(12)

ADA131301

OFFICE OF NAVAL RESEARCH

Contract No. N00014-78-C-0633

Task No. NR 051-690

TECHNICAL REPORT No. UWIS/DC/TR-83/2

Photoluminescent Properties of n-GaAs Electrodes: Applications of the Dead-Layer Model to Photoelectrochemical Cells

by

William S. Hobson and Arthur B. Ellis*

Prepared for Publication

in the

Journal of Applied Physics

Department of Chemistry
University of Wisconsin
Madison, Wisconsin 53706

July 26, 1983

Approved for Public Release: Distribution Unlimited

*To whom all correspondence should be addressed.

REPORT DOCUMENTATION PAGE		READ INSTRUCTIONS BEFORE COMPLETING FORM
1. REPORT NUMBER UWIS/DC/TR-83-2	2. GOVT ACCESSION NO. AD-A131 301	3. RECIPIENT'S CATALOG NUMBER
4. TITLE (and Subtitle) Photoluminescent Properties of n-GaAs Electrodes: Applications of the Dead-Layer Model to Photo-electrochemical Cells		5. TYPE OF REPORT & PERIOD COVERED 6. PERFORMING ORG. REPORT NUMBER
7. AUTHOR(s) William S. Hobson and Arthur B. Ellis		8. CONTRACT OR GRANT NUMBER(s) N00014-78-C-0633
9. PERFORMING ORGANIZATION NAME AND ADDRESS Department of Chemistry, University of Wisconsin, Madison, Wisconsin 53706		10. PROGRAM ELEMENT, PROJECT, TASK AREA & WORK UNIT NUMBERS NR 051-690
11. CONTROLLING OFFICE NAME AND ADDRESS Office of Naval Research/Chemistry Program Arlington, Virginia 22217		12. REPORT DATE July 26, 1983 13. NUMBER OF PAGES 19
14. MONITORING AGENCY NAME & ADDRESS(if different from Controlling Office)		15. SECURITY CLASS. (of this report) Unclassified 15a. DECLASSIFICATION/DOWNGRADING SCHEDULE

16. DISTRIBUTION STATEMENT (of this Report)

Approved for Public Release: Distribution Unlimited

17. DISTRIBUTION STATEMENT (of the abstract entered in Block 20, if different from Report)

18. SUPPLEMENTARY NOTES

Prepared for publication in the Journal of Applied Physics

19. KEY WORDS (Continue on reverse side if necessary and identify by block number)

photoluminescence, gallium arsenide electrodes, dead-layer model

20. ABSTRACT (Continue on reverse side if necessary and identify by block number)

Single-crystal samples of n-type GaAs have been used as electrodes in photoelectrochemical cells (PECs) employing aqueous ditelluride electrolyte. Photoluminescence (PL) from the electrodes can be quenched by the electric field present in the semiconductor during PEC operation. The extent of PL quenching, studied as a function of carrier concentration, excitation wavelength, and applied potential, is consistent with the dead-layer model previously used to describe PL quenching in semiconductor/metal, Schottky-barrier systems. PL quenching curves calculated by assuming that the

dead-layer thickness varies with applied potential in the same manner as the depletion width differ from the experimental data, particularly in the region near the flat-band potential. Sources of these discrepancies are discussed, including the possibility that relative PL intensity reflects the manner in which applied potential is partitioned across the semiconductor-electrolyte interface.

A

Photoelectrochemical cells (PECs) employing III-V semiconductors have assumed a prominent role in the practical and theoretical development of PECs. Practical developments are illustrated by the large optical (solar) energy conversion efficiencies reported for PECs constructed from n-GaAs[1,2] or ternary n-$GaAs_{1-X}P_X$ ($X \sim 0.4$)[3,4] electrodes and stabilizing aqueous diselenide or ditelluride electrolytes. Theoretical investigations have centered on the development of models for the semiconductor-electrolyte interface. Expectations fostered by the ideal model - maximum open-circuit photovoltages dependent on electrolyte redox potentials, e.g.- are often not realized for the III-V-based PECs and have prompted alternative explanations involving surface states and Fermi-level pinning.[5,6] At issue is the manner in which the electric field varies from the solution Helmholtz layer through the semiconductor's surface and bulk regions and its infuence on interfacial charge-transfer kinetics.

Work in our laboratory has focussed on the luminescent properties of semiconductor electrodes.[7-11] These studies have primarily utilized n-type II-VI semiconductors such as n-CdS_XSe_{1-X} ($0 \leq X \leq 1$) and aqueous polychalcogenide electrolytes. In this paper we report the extension of our studies to stable PECs consisting of n-GaAs electrodes and ditelluride electrolytes. By examining quenching of photoluminescence (PL) in this PEC as a function of carrier concentration, excitation wavelength, and applied potential, we demonstrate that the quenching is consistent with the dead-layer model used to describe PL quenching in semiconductor/metal, Schottky-barrier systems: electron-hole ($e^- - h^+$) pairs formed within some fraction of the depletion width do not contribute to PL.[12-19] Since the dead-layer model relates relative PL intensity to the spatial extent of the electric field in the semiconductor, it may possibly be used to probe the manner in which applied potential is partitioned across the semiconductor-electrolyte interface. This use of PL to characterize interfacial energetics is examined using data acquired for the n-GaAs-based PECs.

The single-crystal samples of n-GaAs employed in these studies possessed carrier concentrations, n, ranging from $\sim 10^{16}$-10^{19} cm^{-3}, as indicated in Table I. Prior to use, the electrodes were etched for 10-20 s in 1:1 (v/v) H_2SO_4/H_2O_2 (30%) at 295K. Ditelluride electrolyte, synthesized as described previously,[3,20] typically had a composition of 7.5 M KOH/0.2 M Te^{2-}/0.001-0.006 M Te_2^{2-}. Potentiostatic experiments were conducted with a standard three-electrode setup (n-GaAs working electrode, saturated calomel reference electrode, and Pt counterelectrode) using cells and electrochemical equipment previously described.[7]

Front-surface PL was monitored during PEC operation by placing the cell in the sample compartment of an emission spectrometer and orienting the semiconductor at $\sim 45°$ to both the incident laser excitation and the emission detection optics.[9] At the three ultraband gap excitation wavelengths employed - 457.9, 514.5 and 632.8 nm - GaAs has absorptivities, α, of $\sim 1.6 \times 10^5$, 0.91×10^5, and 0.44×10^5 cm^{-1}, respectively;[21,22] this range of α permits the effective optical penetration depth to be varied by a factor of nearly four. All of the GaAs samples exhibited PL with uncorrected λ_{max} values of ~ 870 nm, corresponding to roughly the band gap energy of ~ 1.42 eV.[22] Between open circuit (~ -1.4 to -1.7 V vs. SCE) and potentials slightly positive of short circuit (~ -1.0 V vs. SCE), no change in the PL spectral distribution was seen at low resolution, permitting changes in PL to be monitored at a single wavelength, λ_{max}.

The essential feature of the dead-layer model is the division of the semiconductor into a dead-layer zone of thickness D and the bulk region beyond D. Following Sites' treatment, D can be calculated from PL quenching data by use of Eq. (1); like the depletion width W, D is expected to be a function of applied potential, but the two widths are not necessarily equal.[19] In Eq. (1), $\phi_{r_{FB}}$ and ϕ_r are the radiative

$$\frac{\phi_r}{\phi_{r_{FB}}} = \exp(-\alpha' D) \qquad (1)$$

quantum efficiencies at the flat-band potential and at an in-circuit potential; self-absorption is corrected for by $\alpha' = \alpha + \beta$ with β representing the absorptivity for emitted light (for GaAs, $\beta \gtrsim 2\times10^{3}$ cm^{-1} at 870 nm[23]). In applying the dead-layer model to the n-GaAs-based PEC, we will treat the open-circuit potential as being approximately the flat-band potential V_{FB}. We will also make use of the fractional quenching between open circuit and an in-circuit potential, ϕ_{xr}, given by Eq. (2).

$$\phi_{xr} = 1 - \frac{\phi_r}{\phi_{r_{FB}}} \tag{2}$$

Figure 1 presents current-luminescence-voltage (iLV) curves acquired with 514.5-nm light for two extreme GaAs carrier concentrations of $\sim10^{16}$ and 10^{18} cm^{-3}. Photocurrent for both samples has been normalized to a common maximum value in the potential range corresponding to saturation. In this regime, measured values of the photocurrent quantum efficiency ϕ_X for both samples are large ($\sim$0.7) and are probably nearly unity when corrected for solution absorbance and the considerable reflective losses from the mirror-like surfaces. Table I summarizes measured ϕ_X values for the samples of Figure 1 and for several other electrodes with different values of n. With the exception of the electrode with the highest value of n, all exhibit ϕ_X values which are nearly unity for all three excitation wavelengths employed. We attribute the large ϕ_X values for electrodes no. 2-5 to their very substantial diffusion lengths of $\sim2\times10^{-4}$ cm.[24] The electrode with the largest value of n(no. 1) has lower values of ϕ_X, presumably reflecting a smaller diffusion length; a rapid decline in L for $n > 2\times10^{18}$ cm^{-3} has been reported for melt-grown n-GaAs samples.[24]

Most striking in Figure 1 is the fractional quenching of PL intensity which varies strongly with n when measured between open circuit, where the intensities have been arbitrarily matched, and -1.0 V vs. SCE. The more lightly-doped sample with $n \sim 1\times10^{16}$ cm^{-3} exhibits a fractional quenching of $\sim$84%, whereas ϕ_{xr} is only $\sim$11% for $n \sim 1\times10^{18}$ cm^{-3}. Table I summarizes the ϕ_{xr} data and shows that for each excitation wavelength ϕ_{xr} declines as n increases. This trend is consistent with the dead-layer model: larger values of n correspond to smaller thicknesses for

W and D, and less quenching is expected as D shrinks relative to the optical penetration depth. We should point out that the ϕ_X and ϕ_{xr} values of Table I showed little dependence on light intensity over the range of $\sim$0.5-20 mW/cm^2.

Also consistent with the dead-layer model is the dependence of ϕ_{xr} on excitation wavelength. Figure 2 presents iLV curves for a lightly-doped electrode at three excitation wavelengths. Unlike the photocurrent-voltage curves which are virtually superimposable, the PL curves are quite disparate and demonstrate that as the optical penetration depth diminishes and a greater fraction of incident light is absorbed in the dead layer, more quenching obtains. Table I reveals that this trend is exhibited by all of the electrodes examined.

A more quantitative test of the predictions of the dead-layer model can be made by calculating D using Eq. (1) and the Table I data. The expectations that D should decrease with increasing carrier concentration (roughly as $n^{-1/2}$, assuming that D and W have a similar functional dependence) and be independent of excitation wavelength are shown in Table I to be well-satisfied. Approximate values for W have also been included in the table and are comparable to but somewhat larger than corresponding values for D.

Although the Table I data only represent a single in-circuit potential (-1.0 V vs. SCE), we find that the dead-layer model fits our data throughout the potential range of interest. Table II presents calculations of D for a lightly-doped GaAs electrode at $\sim$100-mV intervals between open circuit and -1.0 V. Besides again illustrating their independence of excitation wavelength, values for D also show the expected increase with applied potential. Similar results were obtained for all of the electrodes examined.

Although an assessment of the general applicability of the dead-layer model to PECs awaits investigation of many more systems,[25] it is worthwhile considering potential applications of the model. In principle, field-induced quenching provides a map of the electric field in the semiconductor and might thus be used to determine how applied potential is partitioned across the semiconductor-electrolyte interface. For example, in PECs which conform to the "ideal model", applied potential appears exclusively in the semiconductor and PL intensity should exhibit its maximum dependence on this parameter; at the other extreme, Fermi-level-pinned systems are characterized by the appearance of applied potential exclusively in the Helmholtz region and potential-independent PL intensity is anticipated. The extent to which applied potential is dropped in the depletion region and solution Helmholtz region and the influence of surface states on this distribution of potential has received considerable theoretical attention but has often been difficult to determine experimentally.[6,26,27] The techniques used most extensively for analyzing interfacial energetics have been capacitance and electroreflectance.[28]

We have examined the applicability of PL to characterizing interfacial energetics by comparing experimental PL quenching curves for n-GaAs-based PECs with curves calculated by assuming that all of the applied potential appears in the depletion region; similar comparisons have been made in solid-state systems.[13-18] As approximations, we further assume that D (eq. 1) is proportional to W and that surface recombination velocity, S, does not substantially influence our results; equations for PL intensity which include S as a variable reduce to the simple dead-layer expression of Eq. (1) if S is either relatively independent of potential or relatively large ($S \gg \frac{L}{\tau_p}$ and $\frac{\alpha L^2}{\tau_p}$ where τ_p is the hole lifetime and L is its diffusion length).[21]

With these assumptions, PL quenching is predicted by Eq. (3), where C is a constant such that $D = C(V-V_{FB})^{1/2}$. We calculated C at -1.0 V vs. SCE using

$$\frac{\phi_r}{\phi_{r_{FB}}} = \exp[-\alpha' C(V - V_{FB})^{1/2}] \tag{3}$$

the experimental value of $(V-V_{FB})$ and the value for D; D was calculated by Eq. (1) using the measured value of $\frac{\phi_r}{\phi_{r_{FB}}}$. In the potential regime near short circuit, the value of C appears to be relatively insensitive to modest changes in potential. The constant was then used to calculate $\frac{\phi_r}{\phi_{r_{FB}}}$ as a function of applied bias.

Figure 3 presents a comparison of the calculated and observed PL quenching curves for a PEC constructed from the n-GaAs electrode with n $\sim 4 \times 10^{16}$ cm^{-3}. The two curves, corresponding to 457.9-nm excitation, have been matched at open circuit. Figure 3 reveals that the measured PL curve clearly does not have a functional dependence of the form $\exp[-(V-V_{FB})^{1/2}]$. More specifically, with the assumptions given, less quenching of the open-circuit PL intensity is found than is calculated on the basis of the expected expansion of the depletion width with potential. We find similar results for all of the n-GaAs electrodes employed in this study.

A simple explanation for the discrepancy in the Figure 3 curves is that at potentials near open circuit, which we have approximated here as flat band, applied potential appears predominantly in the Helmholtz layer rather than in the semiconductor. The curves of Figure 3 can, in fact, be roughly matched using the dead-layer model by assuming that $\sim$150 mV of the first 200 mV of potential applied to the electrode falls in the Helmholtz layer; at anodic potentials beyond this point, the additional potential appears exclusively in the semiconductor. A possible explanation for the partitioning of applied potential near flat band may involve surface states. Such behavior has been predicted for semiconductor electrodes possessing a large number of ionized surface states,[26] a criterion likely met by GaAs under our experimental conditions.[29] Potential applied to such electrodes is calculated to drop largely in the Helmholtz region until the Fermi level has reached a position where much of this surface charge no longer remains.[26]

Although the partitioning of applied potential is an appealing explanation for the data of Figure 3, we must emphasize that it is doubtless an oversimplification. Besides neglecting surface recombination velocity effects in analyzing PL quenching, we have also ignored other factors such as electroabsorption effects and potential-dependent back-diffusion of minority carriers into the bulk. Despite these possible complications, the good accord of PL quenching in n-GaAs-based PECs with the dead-layer model is gratifying and suggests that PL for such PECs may well provide a simple, direct way to map the *electric field present* in the semiconductor as a function of applied potential. PL may also prove particularly useful for characterizing PECs not amenable to capacitance or electroreflectance techniques, situations which can arise, e.g., with spatially inhomogeneous semiconductors or with semiconductors having poor surface quality.[10,11,30] Work is in progress in our laboratory to examine both the general applicability of the dead-layer model and the manner in which PL quenching reflects changes in the electric field of semiconductor electrodes.

Acknowledgments

We wish to express our gratitude to Paul Friebertshauser of McDonnell-Douglas Astronautics Corp. for supplying us with samples of VPE GaAs. We also thank Laser Diode Laboratories for donating several GaAs wafers. Helpful discussions with Dr. W. Pinson, and Professors J. R. Sites and K. Uosaki are acknowledged. The authors thank the Office of Naval Research and the University of Wisconsin-Madison University-Industry Research Program for support of this research. A.B.E. gratefully acknowledges support as an Alfred P. Sloan Fellow (1981-83).

References

1. K. C. Chang, A. Heller, B. Schwartz, S. Menezes, and B. Miller, Science, 196, 1097 (1977).
2. B. A. Parkinson, A. Heller, and B. Miller, Appl. Phys. Lett. 33, 523 (1978).
3. W. S. Hobson and A. B. Ellis, Appl. Phys. Lett. 41, 891 (1982).
4. High solar energy conversion efficiencies have also been reported for PECs employing n-$GaAs_{1-X}P_X$ electrodes in conjunction with the ferrocene/ferricenium redox couple in acetonitrile. See C. M. Gronet and N. S. Lewis, Nature, 300, 733 (1982).
5. P. A. Kohl and A. J. Bard, J. Electrochem. Soc. 126, 59 (1979).
6. A. J. Bard, A. B. Bocarsly, F.-R. F. Fan, E. G. Walton, and M. S. Wrighton, J. Am. Chem. Soc. 102, 3671 (1980), and references therein.
7. B. R. Karas and A. B. Ellis, J. Am. Chem. Soc. 102, 968 (1980).
8. A. B. Ellis, B. R. Karas, and H. H. Streckert, Faraday Discuss. Chem. Soc. No. 70, 165 (1980).
9. H. H. Streckert, J. Tong, M. K. Carpenter, and A. B. Ellis, J. Electrochem. Soc. 129, 772 (1982).
10. M. K. Carpenter, H. H. Streckert, and A. B. Ellis, J. Solid State Chem. 45, 51 (1982).
11. H. H. Streckert and A. B. Ellis, J. Phys. Chem. 86, 4921 (1982).
12. D. B. Wittry and D. F. Kyser, J. Appl. Phys. 38, 375 (1967). This original discussion of the dead layer was based on cathodoluminescence studies.
13. R. E. Hetrick and K. F. Yeung, J. Appl. Phys. 42, 2882 (1971).
14. U. Langmann, Appl. Phys. 1, 219 (1973).
15. G. K. Volodina, L. I. Gorshkov, G. P. Peka, and V. I. Strikha, J. Appl. Spectrosc. 29, 1077 (1978).

16. K. Ando, A. Yamamoto, and M. Yamaguchi, J. Appl. Phys. 51, 6432 (1981).

17. K. Ando, A. Yamamoto, and M. Yamaguchi, Jpn. J. Appl. Phys. 20, 679 (1981).

18. K. Ando, A. Yamamoto, and M. Yamaguchi, Jpn. J. Appl. Phys. 20, 1107 (1981).

19. R. E. Hollingsworth and J. R. Sites, J. Appl. Phys. 53, 5357 (1982).

20. A. B. Ellis, S. W. Kaiser, J. M. Bolts, and M. S. Wrighton, J. Am. Chem. Soc. 99, 2839 (1977).

21. K. Mettler, Appl. Phys. 12, 75 (1977).

22. D. D. Sell and H. C. Casey, Jr., J. Appl. Phys. 45, 800 (1974).

23. M. D. Sturge, Phys. Rev. 127, 768 (1962).

24. C. J. Hwang, J. Appl. Phys. 40, 3731 (1969).

25. After this work was submitted, Tomkiewicz informed us that he has found that PL from n-CdSe electrodes also conforms to the dead-layer model: M. Tomkiewicz, private communication and Appl. Phys. Lett., in press.

26. M. Green, J. Chem. Phys. 31, 200 (1959).

27. V. A. Myamlin and Y. V. Pleskov, "Electrochemistry of Semiconductors", (Plenum, New York, 1967) pp. 23-149.

28. R. P. Silberstein, F. H. Pollak, J. K. Lyden, and M. Tomkiewicz, Phys. Rev. B. 24, 7397 (1981) and references therein.

29. B. A. Parkinson, A. Heller, and B. Miller, J. Electrochem. Soc. 126, 954 (1979).

30. R. P. Silberstein and M. Tomkiewicz, Appl. Phys. Lett. 42, 58 (1983).

31. G. E. Stillman, C. M. Wolfe, and J. O. Dimmock, in "Semiconductors and Semimetals", edited by R. K. Willardson and A. C. Beer (Academic, New York), Vol. 12 (1977) p. 169.

Table I. PL-Related Properties of n-GaAs-Based PECs.[a]

Electrode No. (n, cm^{-3})[b]	λ_{ex}, nm[c]	ϕ_x[d]	ϕ_{xr}[e]	$D \times 10^8$ cm (Å)[f]	$W \times 10^8$ cm (Å)[g]
1 ($4-8 \times 10^{18}$)	457.9	0.62	0.09	60 [i]	80-110
	514.5	0.44	0.07	80 [i]	80-110
	632.8	0.33	0.07	160 [i]	80-110
2 (1×10^{18})	457.9	0.77	0.15	100	280
	514.5	0.69	0.11	120	280
	632.8	0.75	0.06	120	280
3 (2.5×10^{17})	457.9	0.73	0.46	390	650
	514.5	0.64	0.30	380	650
	632.8	0.65	0.18	430	650
4 (4×10^{16})	457.9	0.76	0.89	1400	1600
	514.5	0.67	0.75	1500	1600
	632.8	0.75	0.48	1400	1600
5 ($0.7-1 \times 10^{16}$)	457.9	0.70	—[h]	—[h]	3300-3900
	514.5	0.69	0.84	2000	3300-3900
	632.8	0.69	0.60	2000	3300-3900

[a] Properties derived from iLV curves of n-GaAs-based PECs. The PECs consisted of a three-electrode potentiostatic setup and ditelluride electrolyte. Vigorous magnetic stirring and a N_2 blanket were used in all experiments.

[b] N-GaAs electrodes used in PECs. Carrier concentrations are given in parentheses. Electrodes 1 and 2 are (100) melt-grown samples from Laser Diode Laboratories doped with Si and Te, respectively. Electrode 3 is a (100) GaAs:Te melt-grown sample from Morgan Semiconductors, Inc. Electrodes 4 and 5 are VPE samples from McDonnell-Douglas Astronautics, Co. with epilayer thicknesses of 2.3 and 25 μm, respectively, on n^+ GaAs substrates. Electrode surface areas exposed to the electrolyte were ∼0.18, 0.30, 0.18, 0.20 and 0.18 cm^2 for electrodes no. 1-5, respectively.

[c]Excitation wavelengths from Ar^+ (457.9, 514.5 nm) and He-Ne (632.8 nm) lasers. Incident intensities of $\sim$0.5-20 mW/cm^2 were used.

[d]Photocurrent quantum efficiency, defined as electrons flowing in the external circuit per photons absorbed. Data were obtained at -1.0 V vs. SCE and are uncorrected for solution absorption and reflective losses. Current densities of $\sim$1-10 mA/cm^2 were measured.

[e]Fractional PL quenching, defined by Eq. (2), between open circuit and -1.0 V vs. SCE. The open-circuit potentials were $\sim$ -1.35, -1.55, -1.75, -1.72, and -1.72 for electrodes no. 1-5, respectively; these potentials were relatively insensitive to light intensity over the $\sim$0.5-20 mW/cm^2 intensity range employed. Error bars in ϕ_{xr} are $\sim\pm 0.02$. PL intensity was monitored at λ_{max}, $\sim$870 nm.

[f]Dead-layer thickness at -1.0 V vs. SCE calculated from Eq. (1) using absorptivities given in the text and the corresponding fractional PL quenching values given in the adjacent column of this table.

[g]Depletion width at -1.0 V vs. SCE calculated by equating open-circuit potentials given in footnote e of this table with V_{FB}, and equating values of n given in the table with N_D. These should be treated as rough values owing to the uncertainties in N_D and V_{FB}. A value of 12.9 was used for the GaAs dielectric constant.[31]

[h]The PL intensity was too weak at this excitation wavelength to obtain reliable data.

[i]There is somewhat greater uncertainty in these values owing to the smaller fractional quenching (ϕ_{xr}) observed.

Table II. Potential Dependence of the Dead-Layer Thickness[a]

Electrode Potential,[b] V vs. SCE	$Dx10^8$ cm (Å)[c] 457.9 nm	514.5 nm	632.8 nm
-1.0	1400	1500	1400
-1.1	1300	1300	1300
-1.2	1100	1100	1100
-1.3	910	910	840
-1.4	670	700	620
-1.5	440	460	460
-1.6	210	240	230
-1.65	120	110	110
-1.72	0	0	0

[a]Dead-layer thickness, D, as a function of potential for n-GaAs electrode no. 4 ($n \sim 4x10^{16}$ cm^{-3}) when used in the PEC described in footnote a of Table I. The iLV data from which the D values in this table are derived are shown in Figure 2.

[b]Potential of the n-GaAs electrode; the open-circuit potential is -1.72 V.

[c]Calculation of dead-layer thickness from Eq. (1) using absorptivities given in the text and the fractional PL quenching (Eq. 2) between open circuit (equated to V_{FB}) and the indicated potential. PL quenching data were obtained using each of the three indicated wavelengths for excitation; changes in PL intensity were monitored at λ_{max} $\sim$870 nm. Current densities are given in Figure 2.

Figure Captions

Figure 1. Relative photocurrent (bottom panel) and PL intensity (top panel) for two n-GaAs electrodes as a function of potential in PECs employing ditelluride electrolyte; the electrodes were excited with 514.5-nm light and their PL signals were monitored at $\lambda_{max} \sim 870$ nm. The solid curves correspond to electrode no. 5 (cf. Table I) with $n \sim 0.7\text{-}1 \times 10^{16}$ cm^{-3} and a surface area of $\sim$0.18 cm^2; a current density at -1.0 V vs. SCE of 4.2 mA/cm^2 was measured (ϕ_X = 0.69). Dashed curves correspond to electrode no. 2 (cf. Table I) with $n \sim 1 \times 10^{18}$ cm^{-3} and a surface area of $\sim$0.30 cm^2; the current density at -1.0 V vs. SCE was $\sim$1.5 mA/cm^2 (ϕ_X = 0.69). Photocurrents for the two electrodes are relative to values at -1.0 V vs. SCE which have been arbitrarily set at 100; PL intensities are likewise relative to open-circuit values of 100. The iLV curves for each electrode were swept simultaneously at 10 mV/s. The electrolyte redox potential, the short-circuit potential, is -1.13 V vs. SCE.

Figure 2. Relative photocurrent (bottom panel) and PL intensity (top panel) as a function of potential and excitation wavelength for an n-GaAs-based PEC employing ditelluride electrolyte; PL intensity was monitored at $\lambda_{max} \sim 870$ nm. Electrode no. 4 with $n \sim 4 \times 10^{16}$ cm^{-3}(cf. Tables I and II) was sequentially irradiated in these experiments by 457.9-, 514.5-, and 632.8-nm light, yielding curves A, B, and C, respectively. PL intensities are relative to open-circuit values which have been arbitrarily set at 100 for all three excitation wavelengths. Photocurrents are relative to their values at -1.0 V vs. SCE which have also been arbitrarily set at 100. Photocurrent densities at -1.0 V vs. SCE from 457.9- 514.5- and 632.8-nm light were 4.7, 4.3, and 8.6 mA/cm^2, respectively, with corresponding calculated ϕ_X values of 0.76, 0.67, and 0.75; the electrode surface area was 0.20 cm^2. The iLV curves for each excitation wavelength were swept simultaneously at 10 mV/s. The electrolyte redox potential was -1.13 V vs. SCE.

Figure 3. Observed (solid curve) and calculated (dashed curve) PL intensity as a function of potential for an n-GaAs-based PEC. The observed curve is that labeled A in Figure 2, and corresponds to electrode no. 4 with $n \sim 4 \times 10^{16} cm^{-3}$ excited by 457.9-nm light. The calculated curve was obtained by using the dead-layer model and assuming that the dead-layer thickness is proportional to the depletion width, as described in the text.

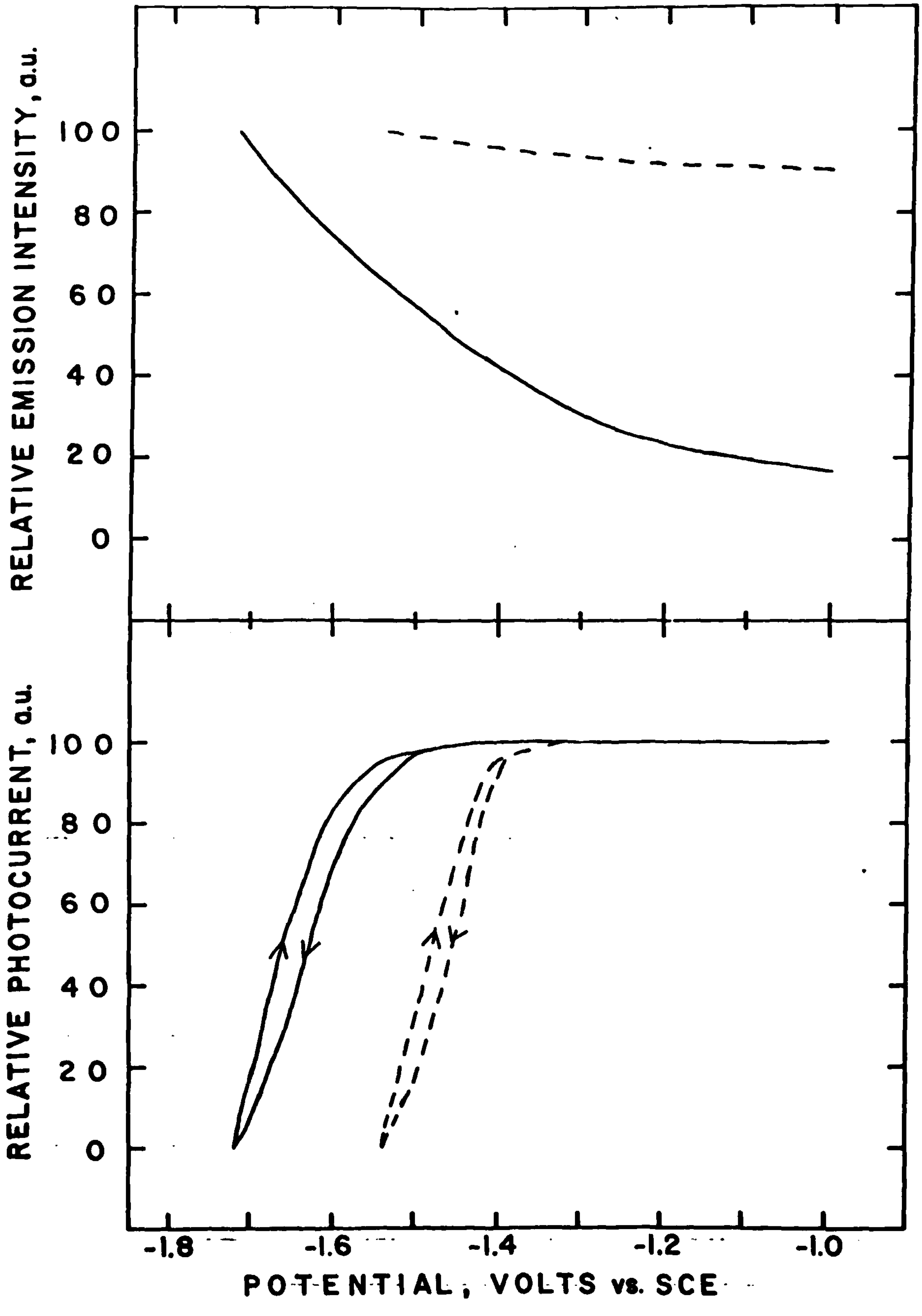
RELATIVE EMISSION INTENSITY, a.u.
100
80
60
40
20
0
RELATIVE PHOTOCURRENT, a.u.
100
80
60
40
20
0
-1.8
-1.6
-1.4
-1.2
-1.0
POTENTIAL, VOLTS vs. SCE

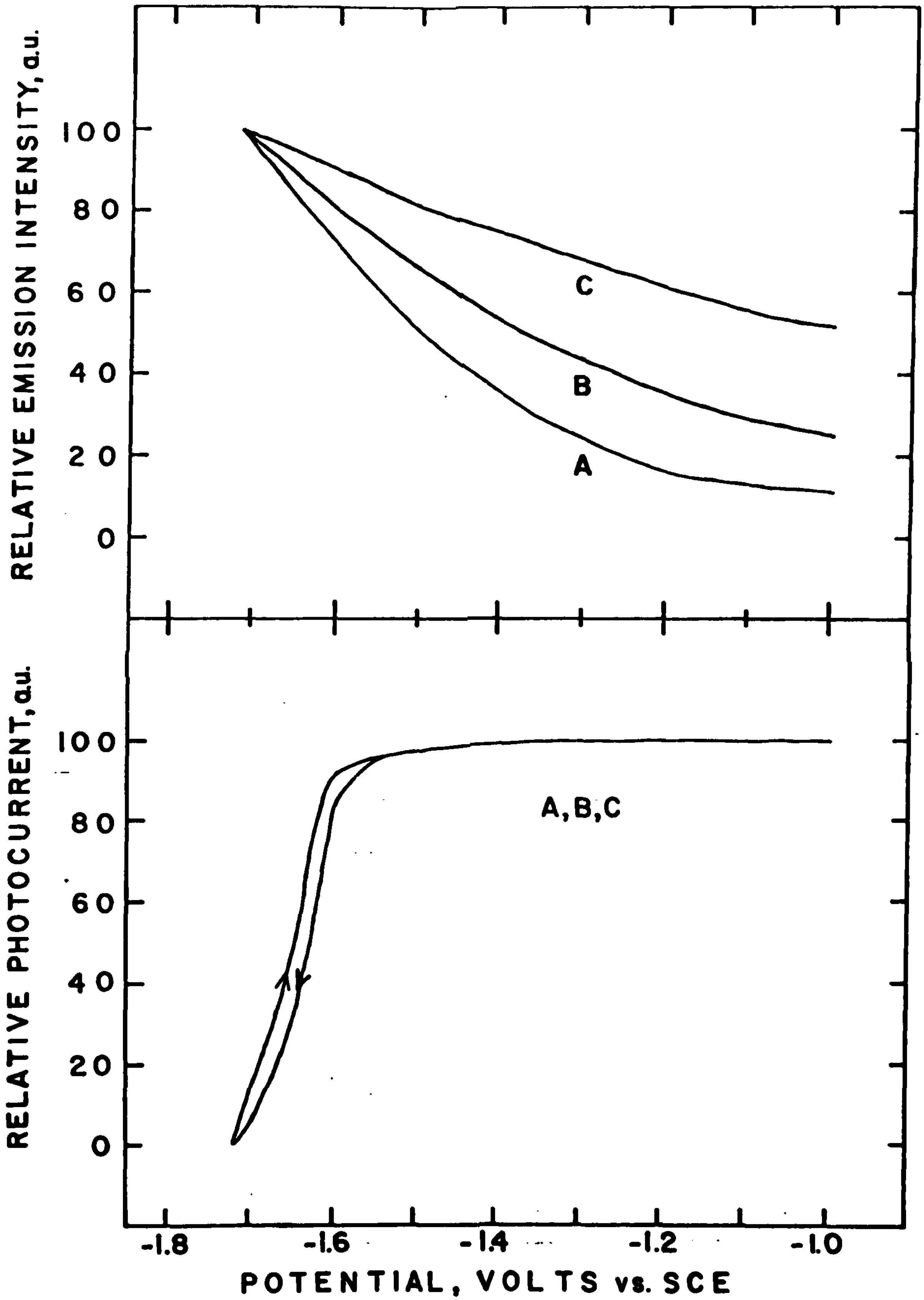
RELATIVE EMISSION INTENSITY, a.u.
100
80
60
40
20
0
C
B
A
RELATIVE PHOTOCURRENT, a.u.
100
80
60
40
20
0
A, B, C
-1.8
-1.6
-1.4
-1.2
-1.0
POTENTIAL, VOLTS vs. SCE

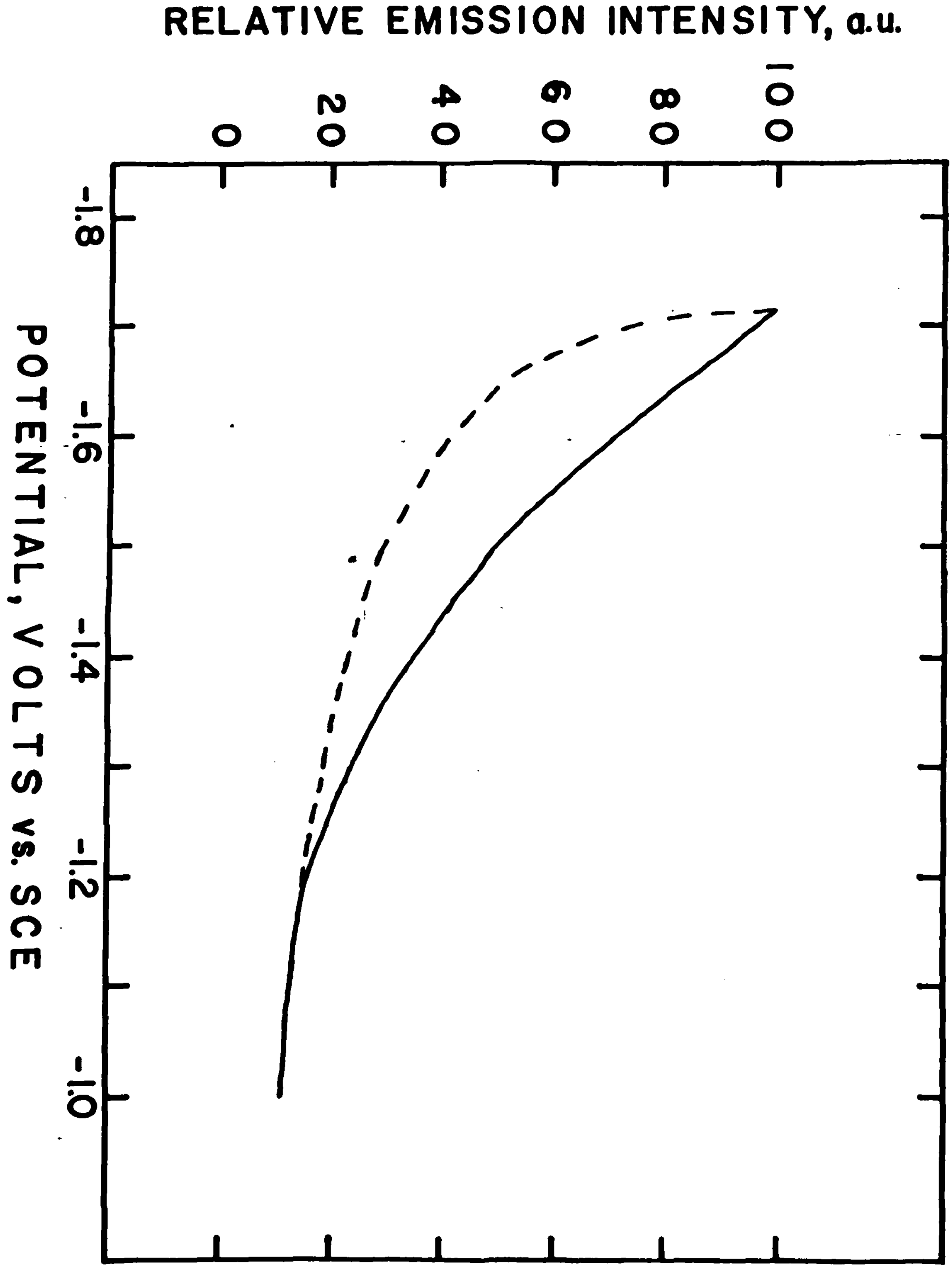
RELATIVE EMISSION INTENSITY, a.u.
0
20
40
60
80
100
-1.8
-1.6
-1.4
-1.2
-1.0
POTENTIAL, VOLTS vs. SCE